ELSEVIER

J. Non-Newtonian Fluid Mech. 152 (2008) 101–112

Journal of Non-Newtonian Fluid Mechanics

www.elsevier.com/locate/jnnfm

Mathematical strategies in the coarse-graining of extensive systems: Error quantification and adaptivity

Markos A. Katsoulakis [a,*], Petr Plecháč [b], Luc Rey-Bellet [c], Dimitrios K. Tsagkarogiannis [d]

[a] *Department of Mathematics, University of Massachusetts, Amherst, USA*
[b] *Mathematics Institute, University of Warwick, Coventry, United Kingdom*
[c] *Department of Mathematics, University of Massachusetts, Amherst, USA*
[d] *Max Planck Institute for Mathematics in the Sciences, Leipzig, Germany*

Received 12 January 2007; received in revised form 17 April 2007; accepted 10 May 2007

Abstract

In this paper we continue our study of coarse-graining schemes for stochastic many-body microscopic models started in Katsoulakis et al. [M. Katsoulakis, A. Majda, D. Vlachos, Coarse-grained stochastic processes for microscopic lattice systems, Proc. Natl. Acad. Sci. 100 (2003) 782–782, M.A. Katsoulakis, L. Rey-Bellet, P. Plecháč, D. Tsagkarogiannis, Coarse-graining schemes and a posteriori error estimates for stochastic lattice systems, M2AN Math. Model. Numer. Anal., in press], focusing on equilibrium stochastic lattice systems. Using cluster expansion techniques we expand the exact coarse-grained Hamiltonian around a first approximation and derive higher accuracy schemes by including more terms in the expansion. The accuracy of the coarse-graining schemes is measured in terms of information loss, i.e., relative entropy, between the exact and approximate coarse-grained Gibbs measures. We test the effectiveness of our schemes in systems with competing short- and long-range interactions, using an analytically solvable model as a computational benchmark. Furthermore, the cluster expansion in Katsoulakis et al. [M.A. Katsoulakis, L. Rey-Bellet, P. Plecháč, D. Tsagkarogiannis, Coarse-graining schemes and a posteriori error estimates for stochastic lattice systems, M2AN Math. Model. Numer. Anal., in press] yields sharp a posteriori error estimates for the coarse-grained approximations that can be computed on-the-fly during the simulation. Based on these estimates we develop a numerical strategy to assess the quality of the coarse-graining and suitably refine or coarsen the simulations. We demonstrate the use of this diagnostic tool in the numerical calculation of phase diagrams.

MSC: 65C05; 65C20; 82B20; 82B80; 82 – 08

Keywords: Coarse-graining; A posteriori error estimate; Adaptive coarse-graining; Relative entropy; Lattice spin systems; Coarse-grained Monte Carlo method; Gibbs measure; Cluster expansion

1. Introduction

Microscopic extended systems with complex and multi-scale interactions are one of the primary quantitative modeling tools in a broad spectrum of scientific disciplines ranging from materials and polymers to biological systems. Such systems are typically simulated by molecular dynamics (MD) or Monte Carlo (MC) methods. However, despite substantial progress in available algorithms, such molecular simulations are typically limited to short length and time scales, compared to device sizes and morphologies observed in experiments. If a reliable coarse-graining method is available, i.e., a new model, derived from the microscopic one, that involves only a reduced number of variables, it can provide a powerful computational tool for speeding-up molecular and multi-scale simulations.

Coarse-graining methods have a long history in the applied sciences and engineering literature. In particular, in polymer science, a sophisticated array of methods have been developed recently, and they are, in spirit, closely related to our proposed methodologies. In the coarse-graining of macromolecules the primary goal is to group together, in a systematic man-

* Corresponding author.
E-mail addresses: markos@math.umass.edu (M.A. Katsoulakis), plechac@maths.warwick.ac.uk (P. Plecháč), lr7q@math.umass.edu (L. Rey-Bellet), tsagkaro@mis.mpg.de (D.K. Tsagkarogiannis).

0377-0257/$ – see front matter © 2007 Elsevier B.V. All rights reserved.
doi:10.1016/j.jnnfm.2007.05.005

ner, several atoms on a macromolecule, creating an effective new chain, as means of reducing the degrees of freedom of the original system, see for instance [31,8,4,10]. Key challenges here include the presence of complex short- and long-range interactions, the off-lattice nature of the models, as well as the typical issues related to the high-dimensional integrations necessary for extensive systems. The integration issue is handled by adopting a semi-empirical strategy that allows the break-up of the computational task into simpler, lower dimensional integrations by assuming some additional structure on the coarse-grained interactions; for instance eliminating multibody terms and assuming a particular form for the coarse-grained bonded and non-bonded interactions. An alternative, statistics-based, approach for the coarse-graining of macromolecules was also developed recently [27]. In this method a parametrization of coarse-grained potentials assumed to be of a known functional form, e.g., Lennard–Jones, is optimized sequentially, against pair distribution functions obtained from atomistic simulations. The reverse procedure of coarse-graining, i.e., reproducing the microscopic properties directly from CG simulations is an issue arising extensively in the polymer science literature [32,27]. The main idea is that computationally inexpensive CG simulations are expected to reproduce the large scale structure; subsequently microscopic information will be added through a process of microscopic reconstruction, reversing the coarse-graining. Mathematical results on error quantification for this issue were first obtained in the context of lattice systems in [18,22].

Although coarse-graining methods can provide a powerful computational tool in molecular simulations, it has been also observed that in some regimes important macroscopic properties may not be captured properly [1,28]. For example, in coarse-grained Monte Carlo (CGMC) simulations for lattice systems, hysteresis and critical behavior are not captured adequately for short and intermediate range potentials, while CGMC performs well in the case of long-range interactions [19,20]. Relying on these observations, we initiate here a systematic study of coarse-graining methods, from the point of view of numerical analysis where error is estimated in view of a specified tolerance.

We restrict ourselves to stochastic (Ising-type) lattice systems as a paradigm of hierarchical coarse-graining because they are, mathematically and computationally, more tractable than, for instance, off-lattice deterministic systems such as in MD. Furthermore, lattice systems are of interest on their own as they are widely used in stochastic modeling and Monte Carlo simulations [24]. Such a system, on a lattice with N sites, is specified by translation invariant microscopic Hamiltonians $H_N(\sigma)$ (σ is the microscopic configuration) and an a priori Bernoulli measure $P_N(d\sigma)$. To coarse-grain we subdivide the lattice into M coarse cells and define a new configuration η given by the total magnetization in each coarse cell. An exact coarse-grained Hamiltonian $\bar{H}_M(\eta)$ is given the renormalization group map [9,15]:

$$\mathrm{e}^{-\beta \bar{H}_M(\eta)} = \int \mathrm{e}^{-\beta H_N(\sigma)} P_N(\mathrm{d}\sigma|\eta), \tag{1.1}$$

where $P_N(\mathrm{d}\sigma|\eta)$ is the probability of having a microscopic configuration σ given a configuration η at the coarse level. However, due to the high-dimensional integration, $\bar{H}_M(\eta)$ cannot be easily calculated explicitly and thus used in numerical simulations. Our perspective is to approximate it by viewing it as a perturbation of a, well-chosen, coarse-grained approximating Hamiltonian $\bar{H}_M^{(0)}$, for instance the one suggested in [17,19](see (2.12) below) or in [13,14] where it was constructed using a wavelet expansion. In [20] we proved that, using a cluster expansion, one can expand $\bar{H}_M(\eta)$ around $\bar{H}_M^{(0)}$:

$$\bar{H}_M(\eta) = \bar{H}_M^{(0)}(\eta) + \bar{H}_M^{(1)}(\eta) + \cdots + \bar{H}_M^{(p)}(\eta) + \mathcal{O}(\epsilon^{p+1}), \tag{1.2}$$

where the correction terms $\bar{H}_M^{(1)}$, $\bar{H}_M^{(2)}\ldots$ can be calculated explicitly. The small parameter ϵ is given in (2.16) and depends on the characteristics of the coarse-graining, the potential and the inverse temperature.

The choice of this first approximation $\bar{H}_M^{(0)}$ is crucial to our method and it should, (i) be computable explicitly, analytically as in [13,17] or numerically and (ii) satisfy good a priori estimate with respect to the microscopic Hamiltonian (see Section 2.2). Cluster expansions are widely used in statistical physics (see e.g., [29] for an overview); in particular the cluster expansions around mean-field models (e.g. [30,5,2,26]) used to analyze critical behavior are conceptually related to ours. Our focus is however more on the computational schemes and related numerical analysis questions.

The error estimates in this paper provide bounds, in terms of relative entropy or information loss, between the exactly coarse-grained Gibbs measure associated with $\bar{H}_M(\eta)$ and the approximate, computable, coarse-grained Gibbs measures obtained by truncating the Hamiltonian in (1.2). Error estimates between measures are natural and useful since the measures determine the most likely configurations observed in simulations and the relative entropy estimates quantify the information compression depending on the truncation level in (1.2).

In [20] we tested our numerical schemes, focusing either short/intermediate- or long-range interactions, assessing the effectiveness of the method, especially in phase transition regimes. We continue here our computational explorations for systems with more complex, combined short- and long-range interactions. Such interactions arise in many realistic microscopic systems, one notable example being in macromolecules discussed earlier and in Section 5 below. We assess the coarse-graining schemes by (a) comparing them to fully resolved numerical simulations, and (b) using an analytically solvable model with short- and long-range interactions due to Kardar [16] as a computational benchmark.

Another consequence of the analysis in [20] is to provide a posteriori estimates on the coarse-graining error, i.e., they can be computed *during* a coarse-grained simulation and are expressed exclusively in terms of the coarse variables η. For instance, for the scheme based on $\bar{H}_M^{(0)}(\eta)$, the a posteriori error (see (1.2)) involves only $\bar{H}_M^{(1,2)}(\eta)$ plus a controlled error of order $\mathcal{O}(\epsilon^{2+1})$. In Section 3 we track, on-the-fly, these a posteriori estimates throughout our simulations. They serve as a diagnostic tool for the quality of the numerical coarse-graining and indicate

whether a given level of coarse-graining produces large error and thus needs to be refined, or whether we can safely use a coarser scale and speed up the simulations. This approach leads to an *a* daptive coarse-graining of the microscopic system which relies on the fact that the coarse-grained schemes in [19,20] form a hierarchy of models allowing a seamless transition between microscopic and coarser resolutions. We demonstrate the advantages of such an adaptative approach in the numerical calculation of phase diagrams for systems with combined short- and long-range interactions. Most of the phase diagram can be constructed with very coarse (inexpensive) simulations, while the critical, phase transition regimes, require finer, even fully resolved simulations. The transitions from finer to coarser scales and back are done on-the-fly, using the a posteriori error computation.

2. Summary of theoretical results

In this section we outline our coarse-graining strategy for lattice models of Ising type and, briefly, review the results on related coarse-garining methods obtained in [20] to which we refer for more details and proofs.

2.1. Microscopic lattice models

Let us consider a spin system on the cubic d-dimensional lattice $\Lambda_N = \{x \in \mathbb{Z}^d; 0 \le x_i \le n-1\}$ with $N = n^d$ lattice sites. At each site $x \in \Lambda_N$, the spin $\sigma(x)$ takes value in $\{-1, +1\}$ and we denote by $\sigma = \{\sigma(x)\}_{x \in \Lambda_N} \in \mathcal{S}_N := \{-1, +1\}^{\Lambda_N}$ a configuration on Λ_N. The Hamiltonian of the system is given by

$$H_N(\sigma) = -\frac{1}{2} \sum_{x \in \Lambda_N} \sum_{y \neq x} J(x-y)\sigma(x)\sigma(y) + h \sum_{x \in \Lambda_N} \sigma(x), \qquad (2.1)$$

where the two-body inter-particle potential J describes the interaction between individual spins and h is an external field. For simplicity we assume that periodic boundary conditions are imposed on the system. The finite-volume equilibrium states of the system are given by the canonical Gibbs measure:

$$\mu_{N,\beta}(\mathrm{d}\sigma) = \frac{1}{Z_N} \mathrm{e}^{-\beta H_N(\sigma)} P_N(\mathrm{d}\sigma), \qquad (2.2)$$

where β is the inverse temperature, Z_N the partition function, and $P_N(\mathrm{d}\sigma)$ is the prior distribution on $\mathcal{S}_N$, is the product measure:

$$P_N(\mathrm{d}\sigma) = \prod_{x \in \Lambda_N} \rho(\mathrm{d}\sigma(x)),$$

where $\rho(\sigma(x) = +1) = \rho(\sigma(x) = -1) = 1/2$ is the distribution of a Bernoulli random variable for each $x \in \Lambda_N$.

2.2. Coarse-graining strategy

We now turn to our coarse-graining strategy which consists of three main steps.

Step 1. *Coarse-graining of the configuration space.* We partition the lattice Λ_N into $M = m^d$ disjoint cells with each cell containing $Q = q^d$ lattice points so that $N = n^d = MQ = m^d q^d$. We define a coarse lattice $\Lambda_N C = \{k \in \mathbb{Z}^d; 0 \le k_i < m-1\}$ and to each $k \in \Lambda_N C$ we associate the coarse cell $\mathcal{C}_k = \{x \in \Lambda_N; qk_i \le x_i < q(k_i+1)\}$. We will refer to Q as the level of coarse-graining ($Q = 1$ corresponds to no coarse-graining).

In each cell $\mathcal{C}_k$ we define a new spin variable $\eta(k) \in \{-Q, -Q+2, \ldots, Q\}$ given by

$$\eta(k) = \sum_{x \in \mathcal{C}_k} \sigma(x),$$

i.e., $\eta(k)$ is the total spin in C_k. The configuration space for the coarse-grained system is $\bar{S}_M \equiv \{-Q, -Q+2, \ldots, Q\}^{\bar{\Lambda}_M}$ and we denote $\eta = \{\eta(k)\}_{k \in \bar{\Lambda}_M}$ a configuration on the coarse lattice $\bar{\Lambda}_M$. It is also convenient to introduce the coarse-graining map $\mathbf{F} : \mathcal{S}_N \to \bar{S}_M$ given by $\mathbf{F}(\sigma) = \eta$ which assigns a configuration on the coarse lattice $\bar{\Lambda}_M$ given a configuration on the microscopic lattice Λ_N. An equivalent coarse-grained variable, which we shall also use later, is

$$\alpha(k) := \mathrm{card}\{x \in \mathcal{C}_k : \sigma(x) = +1\} = \#\{x \in \mathcal{C}_k : \sigma(x) = +1\} \qquad (2.3)$$

which takes values in $\{0, 1, \ldots, Q\}$. The two equivalent coarse variables are related by $\eta = 2\alpha - Q$ or $\alpha = (\eta + Q)/2$.

Step 2. *Coarse-graining of the prior distribution.* The prior distribution P_N on $\mathcal{S}_N$ induces a new prior distribution on $\bar{S}_M$ given by $\bar{P}_M = P_N \circ \mathbf{F}^{-1}$, i.e.,

$$\bar{P}_M(\eta) = P_N(\sigma : \mathbf{F}(\sigma) = \eta).$$

We note two simple, but important facts, which follow immediately from the definition of $\mathbf{F}$.

- The probability measure $\bar{P}_M(\mathrm{d}\eta)$ is a product measure:

$$\bar{P}_M(\mathrm{d}\eta) = \prod_{k \in \bar{\Lambda}_M} \bar{\rho}(\mathrm{d}\eta(k)) \quad \text{with } \bar{\rho}(\eta(k)) = \binom{Q}{\frac{\eta(k)+Q}{2}} \left(\frac{1}{2}\right)^Q.$$

- The conditional probability measure $P_N(\mathrm{d}\sigma|\eta)$ is a product measure:

$$P_N(\mathrm{d}\sigma|\eta) = \prod_{k \in \bar{\Lambda}_M} \tilde{\rho}_{k,\eta(k)}(\mathrm{d}\sigma), \qquad (2.4)$$

where $\tilde{\rho}_{k,\eta(k)}(\mathrm{d}\sigma)$ depends only on $\{\sigma(x)\}_{x \in \mathcal{C}_k}$; for example we have

$$\tilde{\rho}_{k,\eta(k)}(\sigma(x) = 1) = \frac{\eta(k)+Q}{2Q} \quad \text{and}$$

$$\tilde{\rho}_{k,\eta(k)}(\sigma(x) = -1) = \frac{Q-\eta(k)}{2Q}. \qquad (2.5)$$

For a function $f = f(\sigma)$ the corresponding conditional expectation is given by

$$\mathbb{E}[f|\eta] = \int f(\sigma) P_N(\mathrm{d}\sigma|\eta) = \int f(\sigma) \prod_k \tilde{\rho}_{k,\eta(k)}(\mathrm{d}\sigma). \qquad (2.6)$$

Step 3. *Coarse-graining of the Hamiltonian.* We define an *exact* coarse-grained Hamiltonian $\bar{H}_M(\eta)$ by using the renormalization group block averaging transformation (also known as Kadanoff transformation), i.e.,

$$e^{-\beta \bar{H}_M(\eta)} = \mathbb{E}[e^{-\beta H_N}|\eta]. \tag{2.7}$$

Given the Hamiltonian $\bar{H}_M(\eta)$ we define the corresponding Gibbs measure on $\bar{S}_M$ by

$$\bar{\mu}_{M,\beta}(d\eta) = \frac{1}{\bar{Z}_M} e^{-\beta \bar{H}_M(\eta)} \bar{P}_M(d\eta). \tag{2.8}$$

The factor β in front of $\bar{H}_M$ is merely a convention as, in general, the Hamiltonian $\bar{H}_M$ depends itself on β in a nonlinear way. From a practical, and computational, point of view the nonlinear Kadanoff transformation, even for moderately large N, is impossible to compute directly, and our goal is to present a rather systematic way of calculating explicit approximations of the coarse-grained Hamiltonian $\bar{H}_M$, to any given degree of accuracy. Our approach consists of two distinct substeps:

Step 3a. Find a "good" first approximation $\bar{H}_M^{(0)}(\eta)$ for the exact coarse-grained $\bar{H}_M(\eta)$. Since $\bar{H}_M(\eta)$, of course, is unknown, a convenient way to quantify our first approximation is to *require* the following a priori estimate on $\bar{H}_M^{(0)}(\eta)$: If $\mathbf{F}(\sigma) = \eta$ then

$$\frac{\beta}{N}|H_N(\sigma) - \bar{H}_M^{(0)}(\eta)| = O(\epsilon) \tag{2.9}$$

for a suitable chosen small parameter ϵ. We include β on the left hand side of this estimate since β multiplies the Hamiltonian in the Gibbs measure. It is important to note that the choice of $\bar{H}_M^{(0)}(\eta)$ is not given a priori, nor necessarily unique: a good choice of $\bar{H}_M^{(0)}(\eta)$ should take into account all the properties of the system, e.g., temperature, range of the interaction, oscillations of the interactions, and so on. We will discuss one such choice [19,20] and its range of applicability in the next section.

Step 3b. Using the initial approximation $\bar{H}_M^{(0)}(\eta)$ we rewrite the exact coarse-graining as (1.1), or

$$\bar{H}_M(\eta) = \bar{H}_M^{(0)}(\eta) - \frac{1}{\beta} \log \mathbb{E}[e^{-\beta(H_N(\sigma) - \bar{H}_M^{(0)}(\eta))}|\eta]. \tag{2.10}$$

The usefulness of this formula lies in the estimate (2.9), the fact $H_N(\sigma) - \bar{H}_M^{(0)}(\eta)$ is a sum of local interactions, and the fact the conditional probability $P_N(d\sigma|\eta)$ is a product measure at the coarse level. These facts put us, at least in principle, in the domain of applicability of cluster expansion techniques which allow a rigorous expansion of $\bar{H}_M$ in power of ϵ.

Remark 2.1. For fixed N the Kadanoff transformation is always well-defined. However, from a physical point of view, one should be able to construct $\bar{H}_M(\eta)$, for all M, as a sum of translation-invariant local many-body interactions. In this respect it is known that the Kadanoff transformation suffers some relatively mild pathologies at very low temperatures [33,3] but this will not affect our discussion in the parameter ranges where our techniques apply.

2.3. Coarse-grained Hamiltonians and error estimates

We provide a concrete example where the strategy outlined in Section 2.2 has been carried out successfully [20]. In particular it covers the case of system with long-range interactions which is physically relevant and computationally challenging. In a subsequent paper [21] we will discuss another choice of $\bar{H}_M^{(0)}$ which is more adapted for systems with strong competition between short- and long-range interactions.

In order to state our assumptions on the interactions let us consider a function $V : \mathbb{R}^+ \to \mathbb{R}$, such that $V(r) = 0$ for $|r| \geq 1$ and let us assume that potential $J(x - y)$ has the form:

$$J(x-y) = \frac{1}{L^d} V\left(\frac{1}{L}|x-y|\right), \quad x, y \in \Lambda_N, \tag{2.11}$$

so that each site interacts with its neighbors up to a distance of L. The factor $1/L^d$ in (2.11) is a normalization which ensures that the strength of the potential J is essentially independent of L and $\simeq \int |V| dr$. This allows us to consider the interaction range L as an independent parameter of the system.

We define the first approximation $\bar{H}_M^{(0)}(\eta)$ by simply averaging the Hamiltonian H_N over coarse cells, i.e., we set

$$\bar{H}_M^{(0)}(\eta) \equiv \mathbb{E}[H_N|\eta]. \tag{2.12}$$

A simple computation using the conditional probability $P_N(d\sigma|\eta)$ shows that for $x, y \in \mathcal{C}_k$ we have

$$\mathbb{E}[\sigma(x)|\eta] = \frac{\eta(k)}{Q}, \qquad \mathbb{E}[\sigma(x)\sigma(y)|\eta] = \frac{\eta(k)^2 - Q}{Q(Q-1)}. \tag{2.13}$$

Using the factorization property of $P_N(d\sigma|\eta)$ one obtains:

$$\bar{H}_M^{(0)}(\eta) = -\frac{1}{2}\sum_k \sum_{l \neq k} \bar{J}(k-l)\eta(k)\eta(l) - \frac{1}{2}\sum_k \bar{J}(0)(\eta^2(k) - Q) + h\sum_k \eta(k),$$

where

$$\bar{J}(k-l) = \frac{1}{Q^2} \sum_{x \in \mathcal{C}_k, y \in \mathcal{C}_l} J(x-y), \quad \text{for } k \neq l,$$

$$\bar{J}(0) = \frac{1}{Q(Q-1)} \sum_{x,y \in \mathcal{C}_k, y \neq x} J(x-y), \quad \text{for } k = l.$$

In $\bar{H}_M^{(0)}(\eta)$ the potential $J(x - y)$ is replaced by its average over a coarse cell and therefore the error for the potential is proportional to

$$E_{kl}(x-y) := J(x-y) - \bar{J}(k-l), \quad x \in \mathcal{C}_k, y \in \mathcal{C}_l,$$

which measures the variation of the potential $J(x - y)$ over a cell. An estimate on the error is provided by the following lemma, see [20].

Lemma 2.1. (Identification of a small parameter) *Assume that J satisfies (2.11) and $V(r)$ is $\mathcal{C}^1$.*

1. *There exists a constant $C > 0$ such that, if $x \in \mathcal{C}_k$ and $y \in \mathcal{C}_l$, we have*

$$|J(x-y) - \bar{J}(k-l)| \leq 2\frac{q}{L^{d+1}} \sup_{\substack{x' \in \mathcal{C}_k, \\ y' \in \mathcal{C}_l}} \|\nabla V(x'-y')\|. \tag{2.14}$$

2. *There exists a constant $C > 0$ such that, if $\mathbf{F}(\sigma) = \eta$, we have*

$$\frac{1}{N}\left|H_N(\sigma) - \bar{H}_M^{(0)}(\eta)\right| \leq C\frac{q}{L}\|\nabla V\|_\infty. \tag{2.15}$$

While the estimate in Lemma 2.1 is not optimal it adequately identifies a small parameter:

$$\epsilon \equiv C\beta\frac{q}{L}\|\nabla V\|_\infty, \tag{2.16}$$

which encapsulates the various factors influencing our coarse-graining method: (i) ratio q/L of the coarse cell size compared to the interaction range; (ii) temperature; (iii) variations of the potential. Clearly, improved estimates can be obtained when the interaction potential $J(x-y)$ has long-range decay properties.

Using a cluster expansion, the main result proved in [20] is

Theorem 2.2 (Expansion of the Hamiltonian). *Assume that J satisfies (2.11) and that $V(r)$ i s $\mathcal{C}^1$. Then there exists a constant $\delta_0 > 0$ such that if $Q\epsilon < \delta_0$, the Hamiltonian $\bar{H}_M(\eta)$ can be expanded into a convergent series*:

$$\bar{H}_M(\eta) = \sum_{p=0}^{\infty} \bar{H}_M^{(p)}(\eta).$$

where each term $\bar{H}_M^{(p)}(\eta)$ is a sum of finite-range translation-invariant many-body potentials and we have the following error bounds, uniformly in η and N:

$$\frac{\beta}{N}(\bar{H}_M(\eta) - \bar{H}_M^{(0)}(\eta) + \cdots + \bar{H}_M^{(p)}(\eta)) = \mathcal{O}(\epsilon^{p+1}).$$

It is important to note that the theorem provides an algorithm to compute the corrections, in principle, to any degree of accuracy. The first few terms have been calculated explicitly in [20] and are reproduced below.

While Theorem 2.2 gives error bounds at the level of the Hamiltonian, it is important to have error bounds for the corresponding Gibbs measure, since the latter determines the most probable states η. Truncating the expansion we obtained the following Gibbs measures:

$$\bar{\mu}_{M,\beta}^{(p)}(\mathrm{d}\eta) = \frac{1}{\bar{Z}_M^{(p)}} \mathrm{e}^{-\beta(\bar{H}_M^{(0)}(\eta) + \cdots + \bar{H}_M^{(p)}(\eta))} \bar{P}_M(\mathrm{d}\eta).$$

Coarse-graining is an information compression and therefore it is natural to measure errors in this context in terms of the relative entropy which, by definition, is a measure of the information loss. Recall that for two probability distribution π_1 and π_2 defined on a common finite state space $\mathcal{S}$, the relative entropy of π_1 with respect to π_2 is defined as

$$\mathcal{R}(\pi_1|\pi_2) = \sum_{\sigma \in \mathcal{S}} \pi_1(\sigma) \log \frac{\pi_1(\sigma)}{\pi_2(\sigma)}.$$

Furthermore, since we are dealing with extended systems and and compressing local interactions, the errors will be extensive quantities and it is thus natural to measure the error per unit volume, i.e., in terms of the relative entropy per unit volume. Note that the exactness of the coarse-graining given by the Kadanoff transformation is expressed by the fact that (see [20] Section 1.3):

$$\frac{1}{N}\mathcal{R}(\bar{\mu}_{M,\beta}|\mu_{N,\beta} \circ \mathbf{F}^{-1}) = 0.$$

Using Theorem 2.2 one can prove the following estimates [20]:

Theorem 2.3 (Relative entropy error bounds).

$$\frac{1}{N}\mathcal{R}(\bar{\mu}_{M,\beta}^{(0)}|\mu_{N,\beta} \circ \mathbf{F}^{-1}) = \mathcal{O}(\epsilon^2),$$
$$\frac{1}{N}\mathcal{R}(\bar{\mu}_{M,\beta}^{(p)}|\mu_{N,\beta} \circ \mathbf{F}^{-1}) = \mathcal{O}(\epsilon^{p+1}),$$

where $p = 2 \ldots$ and ϵ is given by (2.16).

Note that, naively, one would expect the error for the measure $\bar{\mu}^{(0)}$ constructed with the first approximation $\bar{H}_M^{(0)}$ given in (2.12) to be $\mathcal{O}(\epsilon)$. The fact that it is actually $\mathcal{O}(\epsilon^2)$ is due to cancellations which follow from the definition of $\bar{H}_M^{(0)}$.

2.4. Numerical coarse-graining schemes

Using the Hamiltonians provided by Theorem 2.2 we can construct a number of Monte Carlo methods, at the coarse level, to simulate the Gibbs measure $\mu_{N,\beta}$. We will use Metropolis-type algorithms in this paper, but other choices such as Arhenius dynamics can be used too.

The first scheme is based on the approximation based on $H_M^{(0)}$ and has been extensively studied in [17–19,22].

Scheme 2.1 (Second-order coarse-graining). *The second-order coarse-graining algorithm has the following characteristics*:

1. *Hamiltonian*: $\bar{H}_M^{(0)}$, *see* Eq. (2.12).
2. *Gibbs measure*: $\bar{\mu}_{M,\beta}^{(0)}(\mathrm{d}\eta) = \frac{1}{\bar{Z}_M^{(0)}} \mathrm{e}^{-\beta\bar{H}_M^{(0)}(\eta)} \bar{P}_M(\mathrm{d}\eta)$.
3. *Relative entropy error*: $\frac{1}{N}\mathcal{R}(\bar{\mu}_{M,\beta}^{(0)}|\mu_{N,\beta} \circ \mathbf{F}^{-1}) = \mathcal{O}(\epsilon^2)$.

Thus the scheme is second-order accurate.

Our second scheme is based on the expansion of the Hamiltonian in Theorem 2.2 and the error is $\mathcal{O}(\epsilon^3)$.

Scheme 2.2 (Third-order coarse-graining). *The third-order coarse-graining algorithm has the following characteristics*:

1. *Hamiltonian*: $\bar{H}_M^{(0)} + \bar{H}_M^{(1)} + \bar{H}_M^{(2)}$.
2. *Gibbs measure*: $\bar{\mu}_{M,\beta}^{(2)}(\mathrm{d}\eta) = \frac{1}{\bar{Z}_M^{(2)}} \mathrm{e}^{-(\bar{H}_M^{(0)} + \bar{H}_M^{(1)} + \bar{H}_M^{(2)})} \bar{P}_M(\mathrm{d}\eta)$.

3. *Relative entropy error*: $\frac{1}{N}\mathcal{R}(\bar{\mu}^{(2)}_{M,\beta}|\mu_{N,\beta}\circ\mathbf{F}^{-1}) = \mathcal{O}(\epsilon^3)$.

Thus the scheme is third-order accurate.

To provide explicit formulas for $\bar{H}^{(1)}_M$ and $\bar{H}^{(2)}_M$ it is convenient to express our results in terms of the variables $\alpha(k)$, i.e., the number of spins $\sigma(x) = 1$ in the coarse cell $\mathcal{C}_k$, and $\omega(k) = q - \alpha(k)$. We introduce the following quantities, assuming in each case that all spins belong to a single cell but are located at different sites of the cells:

$$E_1(\alpha) := \mathbb{E}[\sigma(x)|\alpha] = \frac{2\alpha - q}{q} \tag{2.17}$$

$$E_2(\alpha) := \mathbb{E}[\sigma(x)\sigma(y)|\alpha] = \frac{\alpha(\alpha-1) - 2\alpha\omega + \omega(\omega-1)}{q(q-1)} \tag{2.18}$$

$$\begin{aligned} E_3(\alpha) :&= \mathbb{E}[\sigma(x)\sigma(y)\sigma(z)|\alpha] \\ &= \frac{\begin{array}{r}\alpha(\alpha-1)(\alpha-2) - 3\alpha(\alpha-1)\omega + 3\alpha(\omega-1)\omega \\ -(\omega-2)(\omega-1)\omega\end{array}}{q(q-1)(q-2)} \end{aligned} \tag{2.19}$$

$$\begin{aligned} E_4(\alpha) :&= \mathbb{E}[\sigma(x)\sigma(y)\sigma(z)|\alpha] \\ &= \frac{\alpha(\alpha-1)(\alpha-2)(\alpha-3) - 4\alpha(\alpha-1)(\alpha-2)\omega}{q(q-1)(q-2)(q-3)} \\ &\quad + \frac{\begin{array}{r}6\alpha(\alpha-1)(\omega-1)\omega - 4\alpha(\omega-2)(\omega-1)\omega \\ +\omega(\omega-1)(\omega-2)(\omega-3)\end{array}}{q(q-1)(q-2)(q-3)} \end{aligned} \tag{2.20}$$

Furthermore, we introduce the notation:

$$j^1_{kl} := \sum_{\substack{x\in\mathcal{C}_k \\ y\in\mathcal{C}_l}} (J(x-y) - \bar{J}(k,l))^2 \tag{2.21}$$

$$j^2_{kl} := \sum_{\substack{x\in\mathcal{C}_k \\ y,\,y'\in\mathcal{C}_l}} (J(x-y) - \bar{J}(k,l))(J(x-y') - \bar{J}(k,l)) \tag{2.22}$$

$$\begin{aligned} j^2_{k_1k_2k_3} :&= \sum_{\substack{x\in\mathcal{C}_{k_1} \\ y\in\mathcal{C}_{k_2},\,z\in\mathcal{C}_{k_3}}} (J(x-y) - \bar{J}(k_1,k_2))(J(y-z) \\ &\quad - \bar{J}(k_2,k_3)) \end{aligned} \tag{2.23}$$

If $k_1 = k_2$ then we also impose that for $x, y \in \mathcal{C}_{k_1}$ we have $y \neq x$.

Then we have

$$\begin{aligned} -\bar{H}^{(1)}_M(\eta) = \frac{\beta}{8}\sum_k 4j^2_{kk}[-E_4(\alpha(k)) + E_2(\alpha(k))] \\ +2j^1_{kk}[E_4(\alpha(k)) + 1 - 2E_2(\alpha(k))] \\ +\frac{\beta}{2}\sum_{k<l} j^1_{kl}[E_2(\alpha(k))E_2(\alpha(l)) \\ -E_2(\alpha(l)) - E_2(\alpha(k)) + 1] + j^2_{kl}[-2E_2(\alpha(k))E_2(\alpha(l)) \\ +E_2(\alpha(k)) + E_2(\alpha(l))] \\ +\frac{\beta}{2}\sum_{k,l\neq k} j^2_{kkl}[-E_3(\alpha(k))E_1(\alpha(l)) \\ +2E_1(\alpha(k))E_1(\alpha(l)) - E_3(\alpha(l))E_1(\alpha(k))]. \end{aligned} \tag{2.24}$$

and

$$\begin{aligned} \bar{H}^{(2)}_M(\eta) = \beta\sum_{k_1}\sum_{k_2>k_1}\sum_{k_3>k_2} j^2_{k_1k_2k_3}[-E_1(\alpha(k_1))E_2(\alpha(k_2)) \\ \times E_1(\alpha(k_3)) + E_1(\alpha(k_1))E_1(\alpha(k_3))] \\ +j^2_{k_2k_3k_1}[-E_1(\alpha(k_2))E_2(\alpha(k_3))E_1(\alpha(k_1)) \\ +E_1(\alpha(k_2))E_1(\alpha(k_1))] \\ +j^2_{k_3k_1k_2}[-E_1(\alpha(k_3))E_2(\alpha(k_1))E_1(\alpha(k_2)) \\ +E_1(\alpha(k_3))E_1(\alpha(k_2))]. \end{aligned} \tag{2.25}$$

3. A posteriori estimation and adaptive coarse-graining

The error estimate in Theorem 2.3, along with the cluster expansion in Theorem 2.2 combine to provide us with an explicit representation of the error in the coarse-grained numerical approximation. For instance, in [20] we showed the following a posteriori error for Scheme 2.1:

Theorem 3.1 (A posteriori error). *We have*

$$\begin{aligned} &\frac{1}{N}\mathcal{R}(\bar{\mu}^{(0)}_{M,\beta}|\mu_{N,\beta}\circ\mathbf{F}^{-1}) \\ &\quad = \frac{1}{N}\mathbb{E}_{\bar{\mu}^{(0)}_{M,\beta}}[R(\eta)] + \frac{1}{N}\log(\mathbb{E}_{\bar{\mu}^{(0)}_{M,\beta}}[\mathrm{e}^{R(\eta)}]) + \mathcal{O}(\epsilon^3), \end{aligned}$$

where the residuum operator R is given by $R(\eta) = \bar{H}^{(1)}_M(\eta) + \bar{H}^{(2)}_M(\eta)$.

Note also that such an *a posteriori* error cannot be numerically computed directly from the relative entropy formula, since it involves the calculation of the entire probability densities. However, the error representation indicates that the error in coarse-graining can be computed on-the-fly, during a coarse-grained simulation. As the theorem suggests, when using Scheme 2.1, the a posteriori error can be described exclusively in terms of the coarse observables η: the error involves only $\bar{H}^{(1,2)}_M(\eta)$ plus a controlled error of order $\mathcal{O}(\epsilon^3)$.

Earlier work that uses only an upper bound and not the sharp estimate of Theorem 3.1 can be found in [6,7]. These papers are more related in spirit to adaptive finite element methods for PDEs, where a posteriori errors are typically used to construct spatially adaptive coarse-grainings. However, the implementation proved somewhat cumbersome due to the extensive sampling needed in determining the optimal spatially variable

coarse lattice mesh, without excluding the possibility that the methods can be substantially improved.

In this paper we implement the sharp a posteriori estimates of Theorem 3.1, tracking them throughout our simulations. The on-the-fly estimated error serves as a diagnostic tool for the quality of the coarse-grained simulations. It indicates when a particular level of coarse-graining produces excessive error and needs to be refined, or when it can be safely coarsened further in order to speed up the simulation. This approach leads to adaptive coarse-graining of the microscopic system and clearly relies on the fact that the coarse-grained models introduced in [19,20] form a hierarchy of models. The hierarchy includes the microscopic description at the finest level, while it allows for a seamless transition between different resolutions.

We demonstrate the use of such diagnostics and the ensuing adaptive coarse-grainings in the numerical calculation of phase diagrams in systems with combined short- and long-range interactions. In this case it turns out that most of the phase diagram is constructed using coarse levels and hence inexpensive simulations, while the relatively fewer regimes where critical phenomena arise, require finer, or even fully resolved simulations. The transitions from finer to coarser scales and back are done on-the-fly, based on the a posteriori error computation. The refinement or coarsening are govern by the error indicator of Theorem 3.1. We remark that this indicator does not easily relate to the absolute error of a given observable (e.g., magnetization). In the presented simulations a simple strategy has been adopted: the change of the level is controlled by the relative value of the indicator with respect to its maximal value along the simulation path. More elaborate strategies for the error control will be discussed elsewhere.

4. Computational algorithms and numerical experiments

The error estimates presented in Section 2.3 open a new way to evaluate a posteriori the quality of coarse-grained simulations performed with Scheme 2.1 or Scheme 2.2. The a posteriori indicator from Theorem 3.1 is useful for exploring phase diagrams efficiently and refininig the simulation only at critical regions of the parameter space. We demonstrate the properties of Schemes 2.1 and 2.2 on a prototype problem that includes both short- and long-range interactions. Competing short- and long-range interactions appear in diverse applications such as micromagnetics, epitaxial growth or macromolecular systems and their implementation is known to be a difficult computational task. The presented test example, due to Kardar [16], has analytical solutions in one or higher dimensions and exhibits a host of interesting complex behavior including phase transitions, multicritical behavior in the antiferromagnetic regime, as well as crossover from mean-field to nearest-neighbor regimes. The one-dimensional system provides a suitable test bed since the exact (analytical) solutions are known for both the classical Ising system (i.e., the nearest-neighbor interactions only) and the mean-field model (the Curie–Weiss model). We use the exact solutions to ensure that the simulations are not influenced by finite-size effects. In all figures the exact solutions visually coincide with the fully resolved simulations, i.e., $q = 1$. We computed error bars for statistical post-processing, however, they are not displayed in the figures due to their small relative size as compared to the scales of figures.

4.1. Test example: combined short- and long-range interactions [16]

The model combines the classical nearest-neighbor interaction of Ising spins in the external magnetic field with a weak long-range interaction. By adding the long-range, Kac-type interaction we observe transition between the critical behavior of the Ising model and the mean-field model. We briefly describe the formulation of the model and refer the reader to [16] for more details about analysis and various types of phase transitions. The Hamiltonian of the system describes interaction of N spins coupled by a nearest-neighbor interaction of the strength K and a long-range Kac-type potential of the constant strength J/N:

$$\beta H(\sigma) = -\frac{K}{2}\sum_{x}\sum_{|y-x|=1}\sigma(x)\sigma(y) - \frac{J}{2N}\sum_{x}\sum_{y\neq x}\sigma(x)\sigma(y) - h\sum_{x}\sigma(x). \tag{4.1}$$

The technique of central-limit minimization applied in [16] yields, in the thermodynamic limit $N \to \infty$, the minimization problem for the free energy $F(K, J, h)$:

$$F(K, J, h) = \min_{m}\left\{\frac{1}{2}Jm^2 + F_0(K, Jm + h)\right\},$$

where $F_0 = F_0(K, h)$ is the free energy of the nearest-neighbor ($J = 0$) Ising model with interaction strength K and external field h. Using the well-known explicit solution of the one-dimensional nearest-neighbor Ising model we have

$$F(K, J, h) = \min_{m}\left\{\frac{1}{2}Jm^2 - \log[\mathrm{e}^{K}\cosh(h + Jm) + (\mathrm{e}^{2K}\sinh^2(h + Jm) + \mathrm{e}^{-2K})^{1/2}]\right\},$$

or equivalently the magnetization curve is given by the minimizer

$$m_\beta(K, J, h) = \operatorname*{argmin}_{m}\left(\frac{J}{2}m^2 - \log\left[\mathrm{e}^{K}\cosh(h + Jm) + \sqrt{\mathrm{e}^{2K}\sinh^2(h + Jm) + \mathrm{e}^{-2K}}\right]\right). \tag{4.2}$$

A sketch of the phase diagram for $h = 0$ is depicted in Fig. 1. In the plane of parameters K and J, with $h = 0$ there is a line of classical (mean-field) second-order transitions corresponding to $J_c = \mathrm{e}^{-2K}$ terminating at a classical tri-critical point given by $K_t = -1/4\log 3$. The line separates the disordered state (with the mean magnetization $\langle m\rangle = 0$) and the ferromagnetic state. We also plot magnetization curves depending on K for specific values of J indicated in the insets in the phase diagram. To

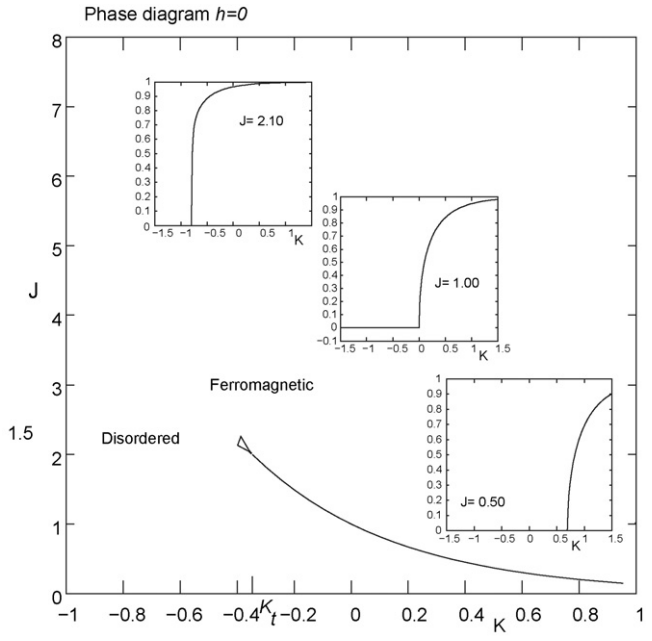

Fig. 1. Phase diagram for the one-dimensional model (the exact solution from [16]). Insets depict depends of the magnetization curve $\langle |m| \rangle$ for the fixed value of J and the fixed external field $h = 0$.

remove degeneracy due to the reflectional symmetry we perform simulations with a small external field $h = 0.05$ and plot the quantity $\langle |m| \rangle$ rather than $\langle m \rangle$. By $\langle \cdot \rangle$ we denote the expected value (average) with respect to the equilibrium Gibbs measure. Knowing the exact solution in the thermodynamic limit we can explore the behavior of the coarse-graining schemes at different regimes, depending on the choice of the parameters K and J.

Case I: long-range interactions only, $K = 0$: First we choose $K = 0$ which corresponds to a purely long-range interaction as in the Curie–Weiss model. The approximation of the hysteresis behavior in coarse-grained simulations provides a good test for the two coarse-graining schemes. It has been observed previously that hysteresis and critical behavior are not captured properly for short and intermediate range potentials [19]. Similar issues in predicting critical behavior were also observed in [28] for coarse-graining of complex fluids. There an artificial solidification effect was observed for higher levels of coarse-graining. Similar issues arise in the coarse-graining of polymer chains [1].

In the numerical tests presented here we demonstrate that the derived corrections improve this behavior even in the case of nearest-neighbor interactions or high coarse-graining ratio q. The sampling of the equilibrium measure is done by using microscopic and coarse-grained Metropolis dynamics. We compute isotherms similarly to natural parameter continuation, i.e., we trace the magnetization m_β versus external field h, first upon increasing the field h from low values and then decreasing it from high values.

While nearest-neighbor Ising models in one dimension do not exhibit phase transitions, for infinitely long attractive interactions there exists a second-order phase transition, and hysteresis behavior is observed according to the global mean-field theory for $\beta > \beta_c$ [12]. More explicitly, the mean-field (Curie–Weiss) model gives the magnetization curve as a solution of the nonlinear equation:

$$m_\beta(h) = \tanh[\beta(J_0 m_\beta(h) + h)]. \tag{4.3}$$

The Curie–Weiss model exhibits phase transition at the critical temperature given by $\beta_c J_0 = 1$ in the case of spins $\{-1, 1\}$ ($\beta_c J_0 = 4$ for spins $\{0, 1\}$). Similarly Ising systems with long enough interaction radii also exhibit phase transitions. We explore two such cases below in the context of our coarse-graining schemes and use the mean-field magnetization (4.3) as a point of reference.

All simulations have been done with the fine lattice of the size $N = 512$. As derived in Theorem 2.2 the errors depend on the interplay of three parameters q, L and β, and the potential J. Improvements due to application of higher-order Scheme 2.2 have been reported in [20]. The transition between two equilibria may not be estimated accurately in the coarse-grained model. The a posteriori error indicator we present here allows us to refine the level of coarse-graining at the critical regions of the phase diagram. This application of the error estimates is demonstrated in Fig. 2 where most of the magnetization curve is simulated at the level $q = 8$ (i.e., coarse-graining to the nearest-neighbor) and it is adaptively refined to capture the transition accurately only at the transition region. In Fig. 3 we also plot the distribution of the error along the continuation in h.

Case II: short-range interactions only, $J = 0$: In this case the test problem reduces to the classical Ising model. We recall that in the case of nearest-neighbor interactions the one-dimensional system does not exhibit phase transition. In fact, the exact solution is given by a well-known formula (see, e.g. [25]), which we adopt to our choice of Hamiltonian with the constant nearest-neighbor ($L = 1$) interaction potential of strength

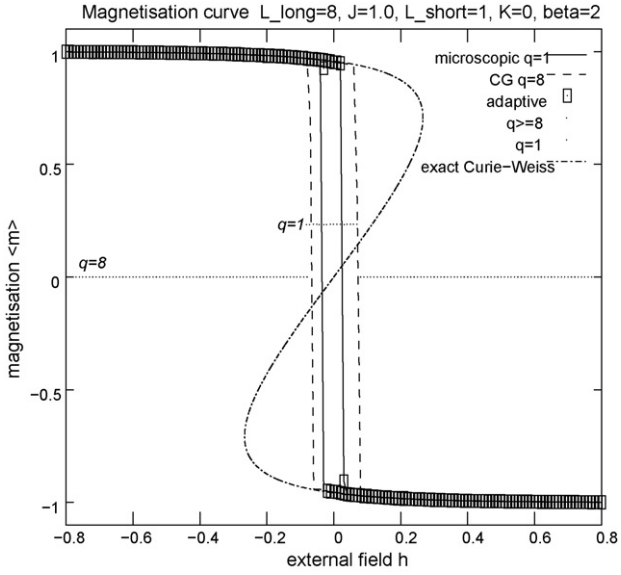

Fig. 2. Demonstration of adaptivity dictated by the a posteriori error indicator. Magnetization curve for the purely long-range interaction case, i.e., $K = 0$. Levels of coarse-graining for sampling at different points of the phase diagram $h - \langle m \rangle$ are depicted in the middle of the figure.

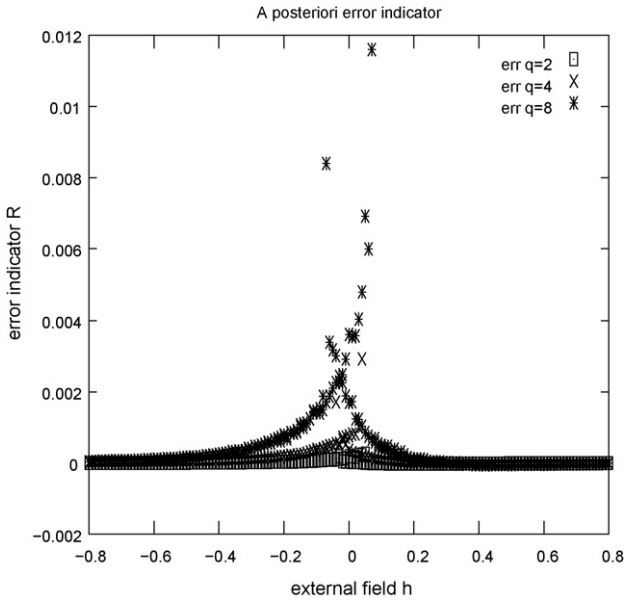

Fig. 3. Distribution of error for the purely long-range interaction case, i.e., $K = 0$.

K. The equilibrium magnetization curve is then given by

$$m_\beta(h) = \frac{\sinh(\beta h)}{\sqrt{\sinh^2(\beta h) + e^{-2\beta K}}}. \tag{4.4}$$

Our analysis predicts that the coarse-graining beyond the interaction range L in this case will produce significant errors. Nonetheless, Fig. 4 demonstrates that including third-order corrections in Scheme 2.2 improves the accuracy for a wide range of interaction strength K. Note that in the Ising model K and β play

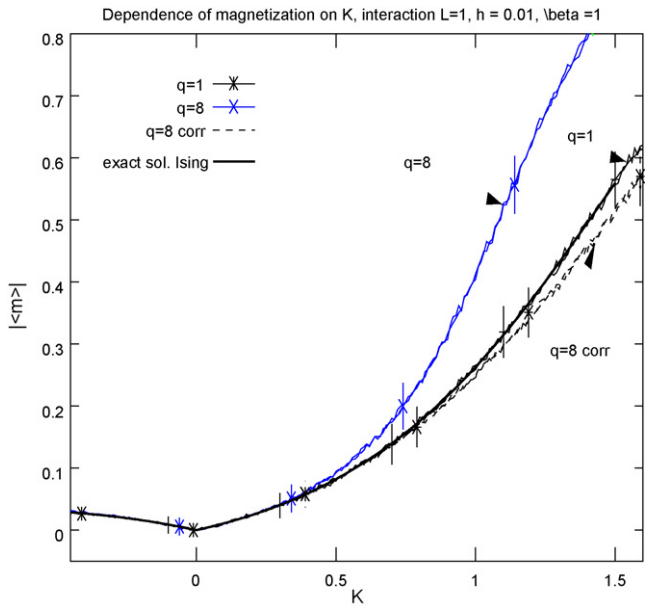

Fig. 4. Magnetization as a function of K for the external field $h = 0.1$ and $\beta = 1.0$. Comparisons of the exact solution (4.4) with fully resolved ($q = 1$) and coarse-grained ($q = 8$) simulations with and without corrections. The interaction range is $L = 1$. Error bars are included in a few points to indicate statistical errors.

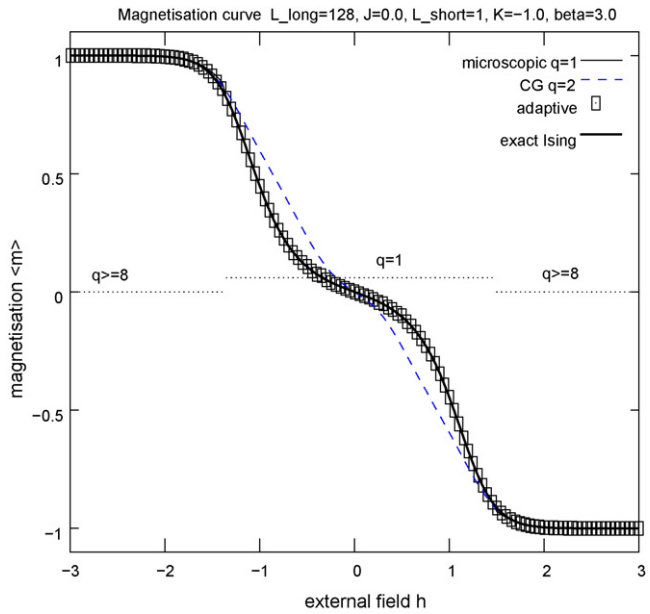

Fig. 5. Magnetization curve for a purely short-range interaction case with the nearest-neighbor antiferromagnetic interaction $K = -1$. Levels of coarse-graining for sampling at different points of the phase diagram $h - \langle m \rangle$ are depicted in the middle of the figure.

an equivalent role. Large values of K correspond to low temperatures. Therefore we include error bars for estimated statistical errors as an accurate sampling in low temperatures becomes more difficult. The discrepancies for higher values of K are consistent with the error estimate in Theorem 2.2. In Fig. 4 we explored also a range of antiferromagnetic interactions, i.e., negative values of K. The exact magnetization curve is again given by (4.4) and is also depicted in Fig. 5. Note that this regime exhibits microstructure (disordered phase) at the finest scale, when the external field h is close to zero; thus the coarse-grained observable η, which is essentially a local average (see Section 2.2), is not expected to work well. We estimate the error using the a posteriori error indicator and Fig. 6 depicts distribution of error along the magnetization curve. When using the error indicator we can explore the phase diagram efficiently as we can limit the region of parameters (h in this case) where fully resolved, microscopic simulations need to be performed. This point is clearly visiaulized in Fig. 5 where we also indicate the level of coarse-graining.

Case III: competing short- and long-range interaction $K \neq 0$ and $J \neq 0$: Many realistic lattice and off-lattice systems arising in diverse applications such as micromagnetics, epitaxial growth or macromolecular systems involve combinations of short- and long-range interactions. We show a comparison of the exact solution (4.2) to coarse-grained simulations in Fig. 7. It appears that both Schemes 2.1 and 2.2 perform modestly well, however a special coarse-graining strategy needs to be devised for such systems due to the short-range interactions in the Hamiltonian. In a subsequent paper [21] we will show how to extend our analysis to such systems with both short- and long-range interactions. However, the presented strategy still allows us to perform simulations with adaptive coarse-graining in which case we can approximate the solution within a controlled error. We observe

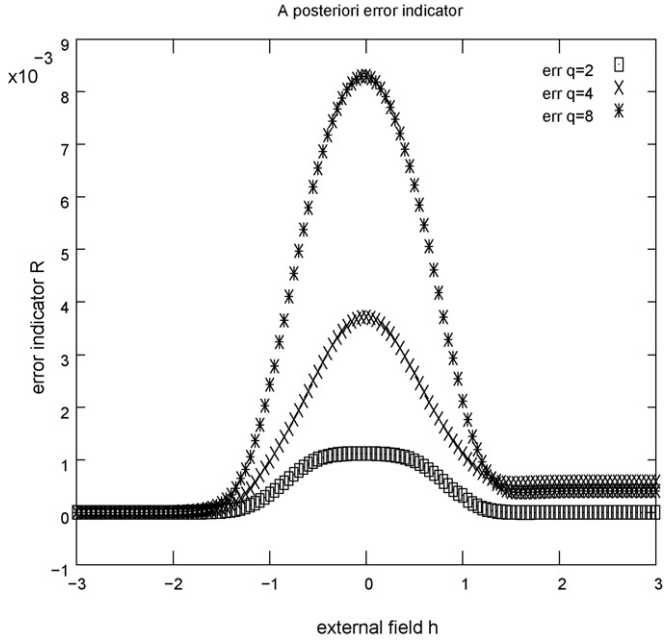

Fig. 6. Distribution of error for purely short-range interaction case with nearest-neighbor antiferromagnetic interaction, i.e., $K = -1$.

in Fig. 7 that depending on the tolerance allowed in the simulation the refinement is not necessarily up to the microscopic level $q = 1$.

We conclude this section with a brief remark about the computational complexity of the approximations. As a simple measure of complexity we use the number of operations required for evaluating the Hamiltonian. Although the actual Monte Carlo step does not require evaluation of the full Hamiltonian the relative complexity with respect to the operation count of the full microscopic simulation $q = 1$ is properly reflected by this measure. The major computational cost in a typical lattice simulation on a d-dimensional lattice will be related to evaluating the long-range interactions of the radius L. We summarize the computational complexity in Table 1 We see that the third-order approximation gives an improved error estimate at the same computational cost whenever $q = L$, in other words, whenever we can compress interactions to the nearest-neighbor potential (Fig. 8).

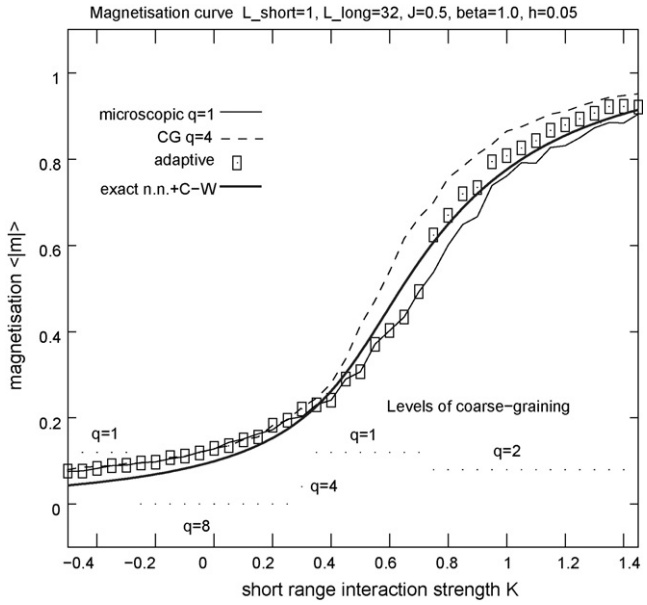

Fig. 7. Adaptive coarse-graining in the computation of the magnetization curve $\langle|m|\rangle$ depending on the strength of the short-range (nearest-neighbor) interaction K. Levels of coarse-graining for sampling at different points of the phase diagram $h - \langle m\rangle$ are depicted in the middle of the figure.

Table 1
Computational complexity of evaluating the Hamiltonian on the d-dimensional lattice for the interaction range L and the coarse-graining level q

	Count	Speed-up
Microscopic $q = 1$: $H_N(\sigma)$	$\mathcal{O}(NL^d)$	1
Scheme 2.1: $\bar{H}_M^{(0)}$	$\mathcal{O}(ML^d/q^d)$	$\mathcal{O}(q^{2d})$
Scheme 2.2: $\bar{H}_M^{(0)} + \bar{H}_M^{(1)}\bar{H}_M^{(2)}$	$\mathcal{O}(ML^{2d}/q^{2d})$	$\mathcal{O}(q^{3d}/L^d)$

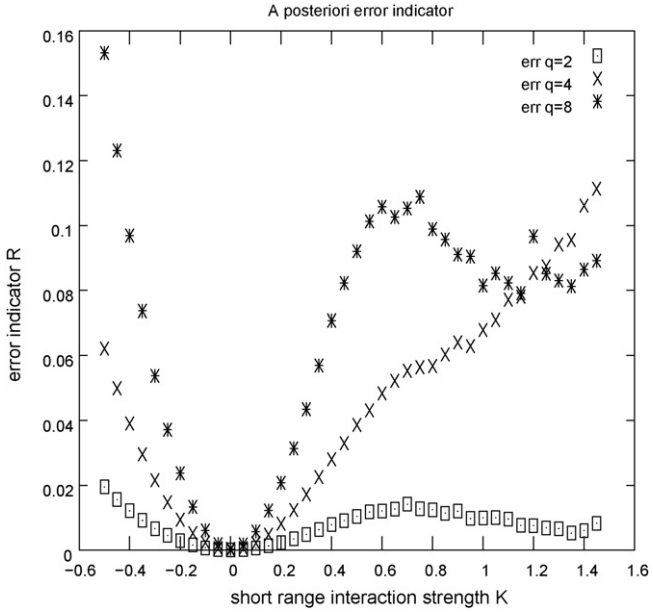

Fig. 8. Distribution of error in computing the K- $\langle|m|\rangle$ phase diagram.

5. Connections to the coarse-graining of polymeric chains

In this paper as well as earlier in [20], we studied analytically and computationally strategies for coarse-graining many-particle microscopic systems. Our work focused on prototype stochastic lattice systems which provide a more tractable set-up to study this problem, while at the same time they can still have complex collective behaviors which pose substantial challenges in devising accurate coarse-graining algorithms. At this point it seems that the our methodologies have the potential to be extended to more complex, off-lattice macromolecular systems. We next briefly outline how such an extension could be carried out by drawing some broad analogies between our current work and existing approaches in polymer science.

Coarse-graining of polymer and other macromolecular systems has attracted considerable attention in polymers science and engineering, [23,27]. The primary goal is to group together in a systematic manner several atoms on a macromolecule, creating an effective new chain, as means of reducing the degrees of freedom of the original system. Some of the key challenges in this effort is the off-lattice set-up of the models, as well as the presence of complex short- and long-range interactions; in fact, the latter feature is what partly motivated our study in Section 4 of lattice systems with combined short- and long-range interactions. Here we consider as our microscopic polymeric system a united atom model, as typically studied in the polymer science coarse-graining literature, see for instance [4,8,10]. This class of models consists of n macromolecules (e.g., polymer chains) in a simulation box with a fixed volume at the inverse temperature β. Each molecule consists of m atoms. We have in total $N = nm$ microscopic particles represented by their position in configuration space $\mathbb{R}^{3d}$, $X = (x_1, \ldots, x_N)$, where $x_i \in \mathbb{R}^3$ is the position vector of the ith atom. The interactions in the system are described by the Hamiltonian:

$$H_N(X) = H_{\mathrm{b}}(X) + H_{\mathrm{nb}}(X) + H_{\mathrm{Coul}}(X) + H_{\mathrm{wall}}(X) + H_{\mathrm{kin}}(X) \tag{5.1}$$

The first term H_{b} defines *short-range* (bonded) interactions between neighboring atoms in each individual polymer chain; it is defined in terms of a potential U_{b}, i.e., $H_{\mathrm{b}} = \sum U_{\mathrm{b}}$ The second term H_{nb} describes non-bonded *long-range* interactions between atoms in different chains and is typically modelled with a Lennard–Jones two-body potential U_{nb}. The Coulomb term H_{Coul} describes interactions associated with charged macromolecules, while H_{wall} interactions with walls. Finally the term H_{kin} is the total kinetic energy of the system. We next consider the canonical Gibbs measure (ensemble) at the inverse temperature β given by

$$\mu(\mathrm{d}X) = Z^{-1} \mathrm{e}^{-\beta H_N(X)} \prod_i \mathrm{d}x_i, \qquad Z = \int_{\mathbf{X}} \mathrm{e}^{-\beta H_N(X)} \prod_i \mathrm{d}x_i. \tag{5.2}$$

In order to obtain a coarse-grained description of the above system, we follow the standard practice in the aforementioned polymer science literature and lump together k microscopic atoms on the same chain into a single coarse-grained state, which is usually referred as a "super-atom"; we thus have $M = N/k$ coarse-grained variables describing the whole system. The coarse variables are denoted by $Q = (q_1, \ldots, q_M)$ where each $q_i \in \mathbb{R}^3$ corresponds to one"super-atom". The new coarse state Q is completely analogous to the coarse variable η employed in the lattice case.

Once the coarse variables are selected, we focus on obtaining the coarse-grained Hamiltonian and the corresponding interaction potentials. In fact, as in the lattice case (2.8), the exact coarse-grained Hamiltonian $\bar{H}_M(Q)$ is defined by the renormalization map:

$$\mathrm{e}^{-\beta \bar{H}_M(Q)} = \int_{\{X | \mathbf{F}X = Q\}} \mathrm{e}^{-\beta H_N(X)} \mathrm{d}X, \tag{5.3}$$

where $\mathbf{F}$ denotes again the projection from fine to coarse variables. Following our strategy outlined earlier for the lattice case, we would next need to identify a suitable first approximation $\bar{H}_M^{(0)}(Q)$ and as in (2.10) rewrite (5.3) as

$$\bar{H}_M(Q) = \bar{H}_M^{(0)}(Q) - \frac{1}{\beta} \log \int_{\{X | \mathbf{F}X = Q\}} \mathrm{e}^{-\beta (H_N(X) - \bar{H}_M^{(0)}(Q))} \mathrm{d}X. \tag{5.4}$$

Cluster expansions can be used to further improve the initial approximation $\bar{H}_M^{(0)}(Q)$, similarly to (1.2).

This outline provides a brief sketch of how the coarse-grained procedure introduced in [20] is extended to off-lattice polymer systems. A detailed presentation, analysis and extensive simulations for the polymers case will appear in [11].

Acknowledgments

The research of M.K. was partially supported by DE-FG02-05ER25702, NSF-DMS-0413864 and NSF-ITR-0219211. The research of P.P. was partially supported by NSF-DMS-0303565. The research or L.R-B. was partially supported by NSF-DMS-0605058. M.K. and P.P. thank Dr. Vagelis Harmandaris for many valuable discussions regarding the coarse-graining of polymer systems.

M.K. and P.P. would like to thank Dr. Vagelis Harmandaris for many illuminating discussions regarding the coarse-graining of polymer systems. The authors also thank the referees for their valuable suggestions.

References

[1] C.F. Abrams, K. Kremer, The effect of bond length on the structure of dense bead-spring polymer melts, J. Chem. Phys. 115 (2001) 2776.
[2] Anton. Bovier, M. Zahradník, The low-temperature phase of Kac–Ising models, J. Stat. Phys. 87 (1–2) (1997) 311–332.
[3] J. Bricmont, A. Kupiainen, R. Lefevere, Renormalization group pathologies and the definition of Gibbs states, Commun. Math. Phys. 194 (1998) 359–388.
[4] W.J. Briels, R.L.C. Akkermans, Coarse-grained interactions in polymer melts: a variational approach, J. Chem. Phys. 115 (2001) 6210.
[5] M. Cassandro, E. Presutti, Phase transitions in Ising systems with long but finite range interactions, Markov Process. Relat. Fields 2 (2) (1996) 241–262.
[6] A. Chatterjee, M. Katsoulakis, D. Vlachos, Spatially adaptive lattice coarse-grained Monte Carlo simulations for diffusion of interacting molecules, J. Chem. Phys. 121 (2004) 11420–11431.
[7] A. Chatterjee, M. Katsoulakis, D. Vlachos, Spatially adaptive grand canonical ensemble Monte Carlo simulations, Phys. Rev. E (2005) 71.
[8] H. Fukunaga, J.J. Takimoto, M. Doi, A coarse-grained procedure for flexible polymer chains with bonded and nonbonded interactions, J. Chem. Phys. 116 (2002) 8183.
[9] N. Goldenfeld, Lectures on Phase Transitions and the Renormalization Group, vol. 85, Addison-Wesley, New York, 1992.
[10] V.A. Harmandaris, N.P. Adhikari, N.F.A. van der Vegt, K. Kremer, Hierarchical modeling of polysterene: from atomistic to coarse-grained simulations, Macromolecules 39 (2006) 6708.

[11] V.A. Harmandaris, M.A. Katsoulakis, P. Plecháč, Coarse-graining schemes for off-lattice interacting particles with internal degrees of freedom, in preparation.
[12] M. Hildebrand, A. Mikhailov, Mesoscopic modeling in the kinetic theory of adsorbates, J. Chem. Phys. 100 (1996) 19089.
[13] A.E. Ismail, G. Rutledge, G. Stephanopoulos, Multiresolution analysis in statistical mechanics. I. Using wavelets to calculate thermodynamics properties, J. Chem. Phys. 118 (2003) 4414–4424.
[14] A.E. Ismail, G. Rutledge, G. Stephanopoulos, Multiresolution analysis in statistical mechanics. II. Wavelet transform as a basis for Monte Carlo simulations on lattices, J. Chem. Phys. 118 (2003) 4424.
[15] L. Kadanoff, Scaling laws for Ising models near t_c, Physics 2 (1966) 263.
[16] M. Kardar, Crossover to equivalent-neighbor multicritical behavior in arbitrary dimensions, Phys. Rev. B 28 (1983) 244–246.
[17] M. Katsoulakis, A. Majda, D. Vlachos, Coarse-grained stochastic processes for microscopic lattice systems, Proc. Natl. Acad. Sci. 100 (2003) 782.
[18] M. Katsoulakis, J. Trashorras, Information loss in coarse-graining of stochastic particle dynamics, J. Stat. Phys. 122 (2006) 115–135.
[19] M.A. Katsoulakis, A.J. Majda, D.G. Vlachos, Coarse-grained stochastic processes and Monte Carlo simulations in lattice systems, J. Comp. Phys. 186 (2003) 250–278.
[20] M.A. Katsoulakis, L. Rey-Bellet, P. Plecháč, D. Tsagkarogiannis, Coarse-graining schemes and a posteriori error estimates for stochastic lattice systems, M2AN Math. Model. Numer. Anal., in press.
[21] M.A. Katsoulakis, P. Plecháč, L. Rey-Bellet, D.K. Tsagkarogiannis, Coarse-graining schemes for lattice systems with short and long range interactions, in preparation.
[22] M.A. Katsoulakis, P. Plecháč, A. Sopasakis, Error analysis of coarse-graining for stochastic lattice dynamics, SIAM J. Numer. Anal. 44 (2006) (6) 2270–2296.
[23] K. Kremer, F. Müller-Plathe, Multiscale problems in polymer science: simulation approaches, MRS Bull. 26 (3) (2001) 205–210.
[24] David P. Landau, Kurt. Binder, A Guide to Monte Carlo Simulations in Statistical Physics, Cambridge University Press, Cambridge, 2000.
[25] D.A. Lavis, G.M. Bell, Statistical Mechanics of Lattice Systems I, Springer-Verlag, 1999.
[26] J.L. Lebowitz, A. Mazel, E. Presutti, Liquid–vapor phase transitions for systems with finite-range interactions, J. Statist. Phys. 94 (5–6) (1999) 955–1025.
[27] F. Müller-Plathe, Coarse-graining in polymer simulation: from the atomistic to the mesoscale and back, Chem. Phys. Chem. 3 (2002) 754.
[28] I.V. Pivkin, G.E. Karniadakis, Coarse-graining limits in open and wall-bounded dissipative particle dynamics systems, J. Chem. Phys. 124 (2006) 184101.
[29] B. Simon, The Statistical Mechanics of Lattice Gases, Vol. I, Princeton Series in Physics. Princeton University Press, Princeton, NJ, 1993.
[30] M. Suzuki, X. Hu, M. Katori, A. Lipowski, N. Hatano, K. Minami, Y. Nonomura, Coherent-Anomaly Method: Mean Field, Fluctuations and Systematics, World Scientific, 1995.
[31] W. Tschöp, K. Kremer, O. Hahn, J. Batoulis, T. Bürger, Simulation of polymer melts. I. Coarse-graining procedure for polycarbonates, Acta Polym. 49 (1998) 61.
[32] W. Tschöp, K. Kremer, O. Hahn, J. Batoulis, T. Bürger, Simulation of polymer melts. II. From coarse-grained models back to atomistic description, Acta Polym. 49 (1998) 75.
[33] A.C.D. van Enter, R. Fernández, A.D. Sokal, Regularity properties and pathologies of position–space renormalization-group transformations: scope and limitations of Gibbsian theory, J. Stat. Phys. 72 (1993) 879–1167.